

## Energy Budget in Rayleigh-Bénard Convection

R. M. Kerr

*National Center for Atmospheric Research, Boulder, Colorado 80307-3000*

*Atmospheric Sciences, University of Arizona, Tucson, Arizona 85721-0081*

(Received 13 March 2001; published 27 November 2001)

It is shown using three series of Rayleigh number simulations of varying aspect ratio AR and Prandtl number Pr that the normalized dissipation at the wall, while significantly greater than 1, approaches a constant dependent upon AR and Pr. It is also found that the peak velocity, not the mean square velocity, obeys the experimental scaling of  $Ra^{0.5}$ . The scaling of the mean square velocity is closer to  $Ra^{0.46}$ , which is shown to be consistent with experimental measurements and the numerical results for the scaling of Nu and the temperature if there are strong correlations between the velocity and temperature.

DOI: 10.1103/PhysRevLett.87.244502

PACS numbers: 47.27.Te, 44.25.+f, 47.27.Eq

This Letter will analyze the energy budget in three-dimensional simulations of Rayleigh-Bénard convection with the objective of testing theoretical assumptions used to explain the laboratory observation of nonclassical heat flux (Nusselt number Nu) exponents in classical turbulent Rayleigh-Bénard convection [1,2]. The budget equation for the average kinetic energy  $q^2/2$  as a function of height  $z$  [3] is

$$\frac{1}{2} \frac{\partial}{\partial t} \overline{q^2} = -\overline{pw}_z - \overline{0.5wq_z^2} + Ra \overline{\omega\theta} + Pr \partial_z^2 \overline{q^2} - Pr \epsilon(z), \quad (1)$$

where shear production  $-\overline{uw(dU/dz)}$  is part of the turbulent production term  $-\overline{0.5wq_z^2}$ . Based upon the observation of strong shears in the boundary layer [4,5] and large-scale flows [6], it was first assumed that the dissipation is primarily concentrated in the boundary layer and is turbulent [7]. More recently it has been suggested that the boundary layer is laminar and the distribution of the total energy dissipation is Rayleigh number dependent [8]. Both of these approaches predict crossovers in scaling behavior. Another theory [9] makes mixing layer assumptions and does not predict these crossovers. The objective in this Letter is to look at the basis for these assumptions by using numerical simulations.

Assuming that  $Nu = \overline{w\theta}/\kappa d \Theta/dz \sim Ra^{\beta_T}$ , the classical exponent is  $\beta_T = 1/3$ , with suggestions since the middle of the 1960s [10,11] that there might be corrections to this exponent. The original experimental result [1] showing that there are significant corrections has recently been extended and refined to give  $Nu \sim Ra^{0.309}$  over nearly ten decades of Rayleigh number Ra [2]. However, detailed experimental information such as budgets cannot be obtained from these large Ra experiments. The only information available besides temperature statistics at a single point is that the Reynolds number based upon vertical velocity fluctuations  $w$  midway up a sidewall proceeds as  $Re = wd/\nu \sim Ra^{1/2}$ . These two observations are incompatible with standard turbulent parametrizations

because the total dissipation is constrained to be  $\epsilon_T = Ra(Nu - 1) \sim Ra^{1.31}$ , while the standard turbulent prediction of  $\epsilon_T = Re^3$  gives  $\epsilon_T \sim Ra^{1.5}$ .

One reason a laminar boundary layer was suggested is that this incompatibility can be resolved if the laminar relationship for dissipation is used,  $\epsilon_T \sim Re^{5/2} \sim Ra^{1.28}$ . This would suggest that convective flows are not filled with cascading eddies, but are instead filled with strong local laminar shears, including a laminar boundary layer. One way to help determine whether the boundary layer is laminar or turbulent is to divide the total energy dissipation  $\epsilon_T$  at some arbitrary boundary layer thickness  $\lambda_{BL}$  into the dissipation in the boundary layers  $\epsilon_{BL}$  and the dissipation in the bulk  $\epsilon_B$ . A new theory for convective scaling [8] has assumed that, in a turbulent boundary layer,  $\epsilon_{BL}$  will be the same order or greater than  $\epsilon_B$ , while if the boundary layer is laminar then  $\epsilon_{BL}/\epsilon_B$  will decrease as Ra increases. This is justified by using the scaling laws above for dissipation in laminar and turbulent boundary layers.

Since the average (or total) dimensionless dissipation  $\epsilon_T = Ra(Nu - 1)$  increases with Ra, it is possible that, even if the boundary layer is laminar at one Ra, an Ra could be reached where the boundary layer becomes unstable and turbulent. Then for higher Ra, as in a shear-driven turbulent boundary layer,  $\epsilon_{BL}/\epsilon_B \rightarrow \text{const}$  would appear.

One way to obtain detailed information such as boundary layer thicknesses and to test these properties is to use simulations. Simulations have reproduced most of the scaling laws and statistical properties of the higher Rayleigh number experiments [12,13], including  $\beta_T$  between 2/7 and 1/3. In a simulation, the thermal boundary layer thickness  $\lambda_T$  can be determined using either  $1/Nu$  or the position of the peak of temperature fluctuations  $\overline{\theta^2}$ . Based upon experience from the analysis of classical shear-driven boundary layers, three definitions of the velocity boundary layer thickness  $\lambda_{BL}$  that can be calculated for convection use the velocity to give  $z^* = 1/Re$ , use the wall shear stress  $\tau = \partial u/\partial x$  to give  $z^+ = \sqrt{\tau}$ , and use the position of the peak of the horizontal velocity fluctuations  $\lambda_u$ , shown in Fig. 3 below. The dimensionless forms have been used in these definitions.

These and additional definitions of the boundary layer thickness could be used to define the dissipation in the boundary layer  $\epsilon_{BL}$ , which we would like to relate to the dissipation at the wall. While  $\epsilon_{BL}$  depends upon the definition of the thickness of the boundary layer, a relationship that could hold for all the definitions above is

$$\epsilon_{BL}/\epsilon_T \leq [\epsilon_W \lambda_{BL}/(d\epsilon_T)], \quad (2)$$

where  $\epsilon_W$  is the dissipation at the wall. This relationship is not very restrictive, but if  $\epsilon_W/\epsilon_T$  were bounded, because  $\lambda_{BL}$  is a decreasing function of  $Ra$  for all the definitions given above,  $\epsilon_{BL}/\epsilon_T$  would be bounded.

In a classical shear-driven boundary layer, all of the definitions of  $\lambda_{BL}$  given above scale with  $Re$  in the same manner. A major difference in convection simulations [12,13] is that each definition of  $\lambda_{BL}$  has a separate power law dependence on  $Ra$ . That is, if

$$\lambda_u \sim Ra^{-\beta_u} \quad \text{and} \quad z^+ = \sqrt{\tau} \sim Ra^{-\beta^+}, \quad (3)$$

then  $\beta_u \approx 1/7$ , and  $\beta^+ > \beta_T$  has been found [12]. Because these results and the theories indicate that  $\lambda_{BL}$  is decreasing rapidly with  $Ra$ , by applying (2) both the turbulent and the laminar boundary layer theories predict that  $\epsilon_W/\epsilon_T$  should increase as  $Ra$  to a power law.

Three simulations have been analyzed to determine the dependence of  $\epsilon_W/\epsilon_T$  upon  $Ra$ . The cases to be discussed are  $AR = 4$  and  $Pr = 0.3$  for  $10^5 < Ra < 10^7$ ,  $AR = 4$  and  $Pr = 7$  for  $10^4 < Ra < 10^7$  from earlier work [14], and  $AR = 1$  and  $Pr = 0.7$  for  $10^6 < Ra < 8 \times 10^7$ , where the Prandtl number  $Pr = \nu/\kappa$  and the aspect ratio  $AR = \text{width}/\text{height}$ . The numerics [13] are pseudospectral, using Chebyshev polynomials in the vertical to provide more resolution and no-slip, constant temperature boundary conditions at the top and bottom walls. In the horizontal, sines and cosines are used to represent free-slip, insulating walls. Profiles will be shown only for the  $AR = 1$  case to save space and because this case is new. The  $AR = 4$  profiles were reported earlier [13].

Previous work [12] demonstrated that  $\epsilon_W$  was much larger than the average dissipation and that  $\epsilon_W/\epsilon_T$  increased with  $Ra$ . Figure 1 shows some of the terms in Eq. (1) for  $AR = 1$ ,  $Pr = 0.7$ , and  $Ra = 8 \times 10^7$ , normalized by  $RaNu$ . For example,  $\epsilon_N(z) = \epsilon(z)/RaNu$ . The  $AR = 4$  cases are similar, except that  $\epsilon_{WN} = \epsilon_W/RaNu$  is smaller,  $\min[\epsilon_N(z)]$  is closer to 1, and  $wq^2/2_{,z}$  is even smaller than here.

While this analysis has confirmed that  $\epsilon_W$  is much larger than the average dissipation and  $\epsilon_W/\epsilon_T$  increases with  $Ra$ , careful examination revealed that there appears to be an upper bound to  $\epsilon_W/\epsilon_T$ , which will be denoted  $\epsilon_{W0}$ .  $\epsilon_{W0}$  is found to be strongly dependent upon  $Pr$  and  $AR$  and lower resolution calculations show that it is converged for each of these cases. Figure 2 demonstrates the approach to the upper bound by plotting the normalized, compensated dissipation at the wall,  $\epsilon_{W0} - \epsilon_{WN}$ . For all three cases,  $\epsilon_{W0} - \epsilon_{WN} \sim Ra^{-0.8 \pm 0.1}$ . While the choice of this particular form is subjective, the consistency in

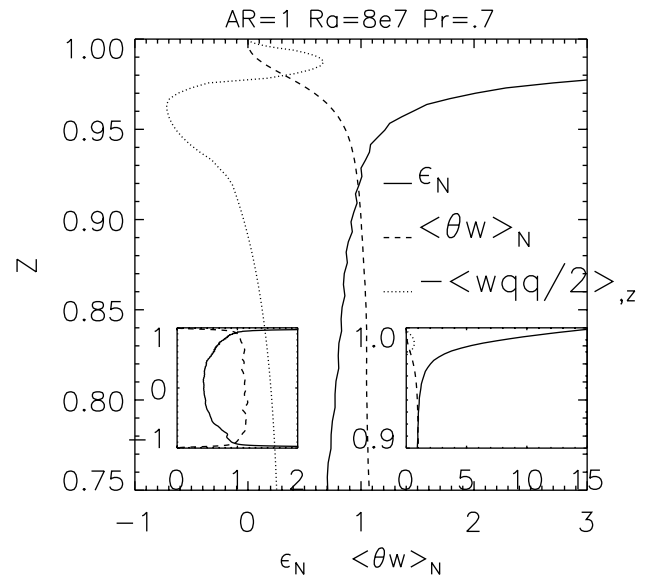


FIG. 1. Production, dissipation, and turbulent transport of kinetic energy from (1) for the simulation  $AR = 1$ ,  $Pr = 0.7$ , and  $Ra = 8 \times 10^7$ . All dimensionless terms are normalized by  $RaNu$  so that the production across the center  $w\theta_N$ , which is also the heat flux, is 1. The insets show production and dissipation through the entire box (height  $d = 2$ ) and very near the wall, where dissipation is very large. The difference between production and dissipation,  $w\theta(z) - \epsilon(z)$ , is the total transport term. As discussed, the pressure transport is close to the difference between the production and dissipation and so is much larger than the turbulent transport  $wq^2/2_{,z}$ .

$\epsilon_{WN} \rightarrow \epsilon_{W0}(AR, Pr)$ , as  $Ra$  grows for all  $AR$  and  $Pr$ , appears to be robust and contradicts the predictions of both the turbulent and laminar boundary layer theories. Because of the bound (2) on  $\epsilon_{BL}$ , then  $\epsilon_{BL}/\epsilon_B \rightarrow 0$  as  $Ra \rightarrow \infty$  at least as fast as

$$\epsilon_{BL}/\epsilon_B < \epsilon_{W0} \lambda_{BL} \sim Ra^{-1/7}, \quad (4)$$

where  $-1/7$  is obtained by using  $\lambda_{BL} = \lambda_u$  from (3).

If this trend were to continue to higher  $Ra$  it would imply that the boundary layer should not be characterized as either a laminar or a turbulent shear-driven boundary layer as has been assumed up to now. Furthermore, it implies that the smallest length scales in the problem are multiples of the Kolmogorov scale  $\eta = \epsilon_T^{-1/4} = [Ra(Nu - 1)]^{-1/4}$ . For example, the wall boundary layer thickness taken from the wall shear stress  $z^+ = \sqrt{\tau}$  should scale as  $\eta$ . If  $\beta_T = 0.309$ , then  $\beta^+ = 0.327$  is predicted.

Now let us consider the mechanisms responsible for transferring energy from the bulk to the boundary layer. This is necessary because Fig. 1 shows that the production of kinetic energy, which is equivalent to the convective heat flux  $w\theta$ , is concentrated in the center of the box, while the peak of the dissipation is at the wall. For there to be a turbulent boundary layer, there would have to be large turbulent production or shear production terms. With the normalization used in Fig. 1,  $w\theta/(RaNu) \approx 1$  in the center and  $\epsilon(z)/(RaNu)$  is slightly less than 1, which is compensated by extra dissipation in the boundary layer.

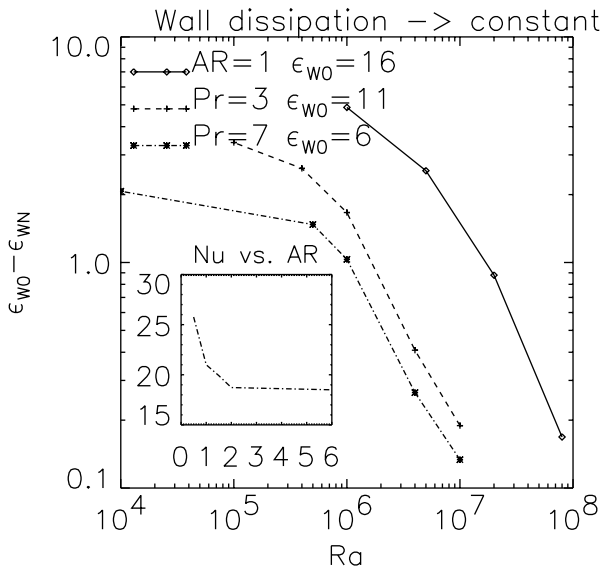


FIG. 2.  $\epsilon_{w0}(\text{AR}, \text{Pr}) - \epsilon_N$  vs  $\text{Ra}$ . The decrease is approximately  $\text{Ra}^{-0.8 \pm 0.1}$  for all three cases (neglecting the lowest  $\text{Ra}$  for  $\text{Pr} = 0.3$  and  $7$ ). The values of  $\epsilon_{w0}(\text{AR}, \text{Pr})$  used are given. The inset shows the dependence on the aspect ratio of  $\text{Nu}$  for  $\text{Ra} = 10^7$  and  $\text{Pr} = 0.7$ .

The three transport terms in (1) that transfer energy from the bulk to the boundary layer are diffusive transport  $\text{Pr} \partial_z^2 q^2$ , the pressure transport  $-\overline{p w_{z,z}}$ , and the turbulent transport  $-0.5 w q_{z,z}^2$ .  $\text{Pr} \partial_z^2 q^2$  and  $-0.5 w q_{z,z}^2$  can be calculated directly while  $-\overline{p w_{z,z}}$  can be calculated from the difference between all the remaining terms. Diffusive transport (not shown) is found to be large only very near the wall, for  $1 - z < 0.02$  in Fig. 1. For  $1 - z < 0.1$  the turbulent transport is much less than the difference between the production and the dissipation, and therefore the turbulent transport is much less than the pressure transport term. This would be consistent with the dissipation in the boundary layer being much less than either the predictions of a turbulent or a laminar boundary layer, both of which depend upon shear production, which is part of the turbulent production term.

The observation that the pressure transport dominates is not new. In the geophysical literature over a wide range in  $\text{Ra}$  beginning at low  $\text{Ra}$  in the laboratory [3] and extended to higher  $\text{Ra}$  in atmospheric observations [14,15], it is found that the primary source of kinetic energy in the boundary layer is the pressure transport term.

If the boundary layer is neither a shear-driven turbulent nor a laminar boundary layer, then what mechanism is responsible for the observed scaling of the velocity scale or Reynolds number  $\text{Re} = w d / \nu$ ? Perhaps the origin is in the details of plume dynamics. It was previously found [16], and confirmed by these simulations, that there is a nearly perfect correlation in the bulk between the vertical velocity  $w$  and temperature fluctuations  $\theta$ , where the total temperature is  $T(x, y, z) = \overline{T}(z) + \theta(x, y, z)$ . What is found everywhere in these calculations, except near the wall ( $z < \lambda_T = d / \text{Nu}$ ), is that

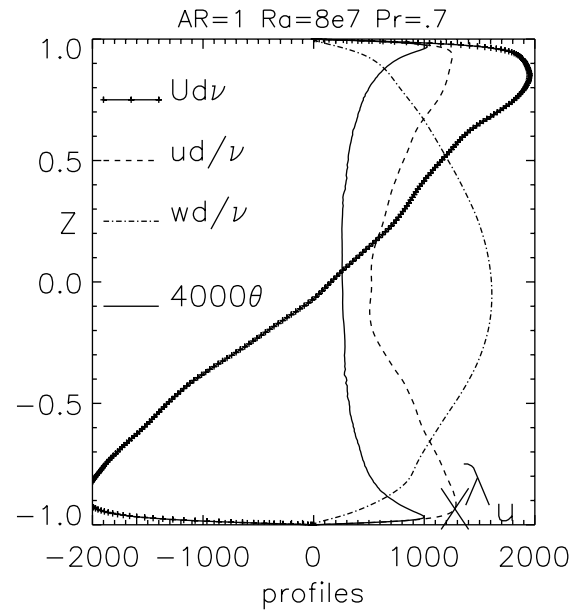


FIG. 3. Reynolds numbers based upon the mean horizontal velocity in the direction of maximum shear  $V d / \nu$ , upon the horizontal fluctuations in velocity  $u d / \nu = (\overline{u^2 + v^2})^{1/2} d / \nu$ , and upon the vertical velocity fluctuations  $w d / \nu$ , for  $\text{AR} = 1$ ,  $\text{Ra} = 8 \times 10^7$ . Also shown is the temperature fluctuation variance  $\overline{\theta^2}^{1/2}$ .

$$\overline{\theta w} \approx 0.9 \overline{w^2}^{1/2} \overline{\theta^2}^{1/2}, \quad (5)$$

where  $\overline{w^2}^{1/2}$  comes from Fig. 3. This would be consistent with visualizations that show small plumes dominating in the boundary layer [5,12,13].

By using (5), it can be predicted that in the center,  $\text{Nu} = \overline{\theta w} / \kappa (d \Theta / dz) \sim \text{Ra}^{\beta_T}$ ,  $\theta' = \overline{\theta^2}^{1/2} \sim \text{Ra}^{-\delta_c}$ , and  $\text{Re} = \overline{w^2}^{1/2} / \nu d \sim \text{Ra}^\gamma$ ,

$$\gamma = \beta_T + \delta_c. \quad (6)$$

The scaling for the simulations and experiments discussed here is given in Table I.  $u d / \nu$  (Fig. 3) is used to determine  $\gamma$  in the simulations. When the experimental values [2] of  $\beta_T = 0.309$  and  $\delta_c = 0.145$  are used, then (6) would predict  $\gamma = 0.454$ , which is the origin of the experimental value given in Table I. However, what is found [17] for the most recent experiment [2] and most earlier experiments [18] is  $\gamma = 0.5$ .

These inconsistencies can be resolved by looking at the scaling of the maximum vertical velocity in the simulations, where it is found that  $\text{Re}_{\text{max}} \sim \text{Ra}^{0.5}$  for all three simulated cases. Furthermore, this maximum is always found roughly midway up a sidewall in a strong persistent plume. Midway up a sidewall is also where the experimental measurements of velocity are taken. Therefore, this indicates that these experimental velocity measurements are not representative of the velocity as a whole, but only representative of the velocity at the walls that probably comes from the maximum possible vertical velocity within plumes. The reason  $\text{AR} = 4$ ,  $\text{Pr} = 7$  gives  $\gamma > 0.5$  can be understood by noting that, even at its

TABLE I. Experimental [2] and numerical exponents. Aspect ratio and Prandtl number for the three numerical cases are given. The experimental value for velocity scaling is given as  $\gamma_{\max}$ . How the experimental value for  $\gamma$  is calculated is explained in the text. Errors for the simulations are based upon the scatter of exponents taken between Ra. Profiles such as Fig. 3 are used to determine  $\beta_T$  and  $\gamma$  for AR = 1 and for the Pr = 0.3 and Pr = 7 cases are taken from previously published curves [13]. Re =  $ud/\nu$  is taken at Ra =  $10^7$  for all three cases.

Cases	Expt.	AR = 1, Pr = 0.7	AR = 4, Pr = 3	AR = 4, Pr = 7
Exp.	Expt.	AR = 1, Pr = 0.7	4,0.3	4,7
$\beta_T$	0.309	$0.27 \pm 0.02$	$0.31 \pm 0.02$	$0.30 \pm 0.02$
$\gamma_{\max}$	0.50	$0.50 \pm 0.01$	$0.50 \pm 0.01$	$0.51 \pm 0.01$
$\delta_c$	0.145	$0.17 \pm 0.02$	$0.14 \pm 0.02$	$0.16 \pm 0.03$
$\gamma$	0.454	$0.46 \pm 0.02$	$0.46 \pm 0.01$	$0.52 \pm 0.03$
Re(Ra = $10^7$ )	...	434	3000	14

highest Ra of  $10^7$ , the Re for this case is not turbulent, and in the published visualizations [13] this case is dominated by laminar plumes. Therefore, the velocity in individual plumes seems to obey  $\gamma_{\max} = 0.5$ , but in the other cases, where the flow is turbulent, the average exponent is closer to  $\gamma = 0.46$ .  $\gamma = 0.46$  could represent an average between  $\gamma_{\max} = 0.5$  and the exponent found for the Reynolds number dependence of the large-scale circulation, where  $\gamma = 0.43$  [19].

It has been found that the dissipation at the wall approaches a multiple of the mean dissipation across the box, contrary to the assumptions of the effect of shear upon the thermal boundary layer. Therefore, it does not seem that the dynamics in the boundary layer can be governed by shears, whether they be laminar or turbulent. Instead, it is suggested that plumes might dominate the dynamics and perhaps a new model of turbulent convection should be constructed based upon plume dynamics. The basis for this suggestion is how the velocity scales. Evidence is presented that the experimentally observed scaling of the Reynolds number as  $\text{Re} \sim \text{Ra}^\gamma$ , with  $\gamma = 0.5$ , can be reproduced by the simulations only if this is taken to be the maximum vertical velocity in persistent plumes along the sidewalls. So one should replace  $\gamma$  by  $\gamma_{\max}$  in the experiments. Based upon the simulations, it is proposed that the simulated exponent based upon the average kinetic energy is  $\gamma \approx 0.46$ , which is shown to be consistent with the experimental measurements of the scaling of the temperature fluctuations and Nu. While the difference between 0.46 and 0.5 for the  $\gamma$ 's is just outside the error bars in the simulations, the correspondence with the experimental observations supports this result. To test this conclusion, a single experiment could measure velocities in several locations, such as near a sidewall, in the interior, and from the large-scale circulation, to determine whether their associated Reynolds numbers scale differently.

NCAR is supported by the National Science Foundation. Conversations with K.R. Sreenivasan, D. Lohse, C. Doering, B. Shraiman, J.R. Herring, and others while the author was a participant in the Program on Hydrody-

namic Turbulence at the Institute for Theoretical Physics, University of California, Santa Barbara, are acknowledged.

- 
- [1] F. Heslot, B. Castaing, and A. Libchaber, Phys. Rev. A **36**, 5870 (1987).
  - [2] J.J. Niemela, L. Skrbek, K.R. Sreenivasan, and R.J. Donnelly, Nature (London) **404**, 837 (2000).
  - [3] J.W. Deardorff and G.E. Willis, J. Fluid Mech. **28**, 675 (1967).
  - [4] J. Werne, Phys. Rev. E **48**, 1020 (1993).
  - [5] G. Zocchi, E. Moses, and A. Libchaber, Physica (Amsterdam) **166A**, 387 (1990).
  - [6] R. Krishnamurti and L.N. Howard, Proc. Natl. Acad. Sci., U.S.A. **78**, 1981 (1981).
  - [7] B.I. Shraiman and E.D. Siggia, Phys. Rev. A **42**, 3650 (1990).
  - [8] S. Grossman and D. Lohse, J. Fluid Mech. **407**, 27 (2000).
  - [9] B. Castaing, G. Gunaratne, F. Heslot, L. Kadanoff, A. Libchaber, S. Thomae, X.Z. Wu, S. Zaleski, and G. Zanetti, J. Fluid Mech. **204**, 1 (1989).
  - [10] P.H. Roberts, *Non-equilibrium thermodynamics and variational techniques and stability analysis* (University of Chicago Press, Chicago, 1965), p. 125; F.H. Busse, Rep. Prog. Phys. **41**, 1930 (1978).
  - [11] J.R. Herring, J. Atmos. Sci. **23**, 672 (1966).
  - [12] R.M. Kerr, J. Fluid Mech. **310**, 139 (1996).
  - [13] R.M. Kerr and J.R. Herring, J. Fluid Mech. **419**, 325 (2000).
  - [14] W.T. Pennell and M.A. Lemone, J. Atmos. Sci. **31**, 1308 (1974).
  - [15] D.H. Lenschow, J.C. Wyngaard, and W.T. Pennell, J. Atmos. Sci. **37**, 1313 (1980).
  - [16] V. Yakhot, Phys. Rev. Lett. **63**, 1965 (1989).
  - [17] J.J. Niemela, L. Skrbek, K.R. Sreenivasan, and R.J. Donnelly, J. Fluid Mech. (to be published).
  - [18] X. Chavanne, F. Chilla, B. Castaing, B. Hebral, B. Chabaud, and J. Chaussy, Phys. Rev. Lett. **79**, 3648 (1997).
  - [19] Sh. Ashkenazi and V. Steinberg, Phys. Rev. Lett. **83**, 3641 (1999); **83**, 4760 (1999).